Computation of action potential propagation and presynaptic bouton activation in terminal arborizations of different geometries

H.-R. Lüscher and J. S. Shiner
Department of Physiology, University of Bern, CH-3012 Bern, Switzerland

ABSTRACT Action potential propagation in axons with bifurcations involving short collaterals with synaptic boutons has been simulated using SPICE, a general purpose electrical circuit simulation program. The large electrical load of the boutons may lead to propagation failure at otherwise uncritical geometric ratios. Because the action potential gradually fails while approaching the branch point, the electrotonic spread of the failing action potential cannot depolarize the terminal boutons above an assumed threshold of 20 mV (V_{rest} = 0 mV) for the presynaptic calcium inflow, and therefore fails to evoke transmitter release even for boutons attached at short collaterals. For even shorter collaterals the terminal boutons can again be activated by the spread of passive current reflected at the sealed end of the bouton which increases the membrane potential above firing threshold. The action potential is then propagated in anterograde fashion into the main axon and may activate the terminal bouton on the other collateral. Differential activation of the synaptic boutons can be observed without repetitive activation of the main axon and with the assumption of uniform membrane properties. Axon enlargements above a critical size at branch points can increase the safety factor for propagation significantly and may serve a double function: they can act both as presynaptic boutons and as boosters, facilitating invasion of the action potential into the terminal arborizations. The architecture of the terminal arborizations has a profound effect on the activation pattern of synapses, suggesting that terminal arborizations not only distribute neural information to postsynaptic cells but may also be able to process neural information presynaptically.

INTRODUCTION

From theoretical and experimental work it has long been recognized that axons might be more than simple transmission lines conveying information faithfully from one part of the nervous system to an other part. As early as 1935 Barron and Matthews suggested that axons may not always conduct the nervous impulse but may modulate the spatial and temporal relations between action potentials. Frequency-dependent conduction failure at axon bifurcations and geometric axon inhomogeneities have been observed in a number of preparations. Failure of neuromuscular transmission during high-frequency stimulation has been shown to originate from the failure of propagation into nerve terminals (Krnjević and Miledi, 1959; Parnas, 1972; Hatt and Smith, 1976; Grossman et al., 1979*a*; Smith, 1980, 1983*b*; Schiller and Rahamimoff, 1989). Failure of impulse conduction has also been observed in the central nervous system of invertebrates and vertebrates (Kennedy and Mellon, 1964; Parnas et al., 1969; Van Essen, 1973; Yau, 1976; Spira et al., 1976; Macagno et al., 1987; Deschênes and Landry, 1980). These experimental observations have stimulated a number of theoretical papers on the effect of changes in core conductor geometry and myelinization on impulse conduction and spike configuration (Khodorov et al., 1969; Goldstein and Rall, 1974; Revenko et al., 1973; Brill et al., 1977; for reviews see Waxman, 1972, 1975; Swadlow et al., 1980). The observation that impulses might be conducted preferentially into only one daughter branch was of special interest, because such branch points may act as frequency-dependent spatial filters (Parnas, 1972; Grossman et al., 1979*a* and *b*; Parnas and Segev, 1979; Stockbridge 1988*a* and *b*). All these observations have suggested that conduction failure and its relief may be used by the central nervous system as a means of processing neural information (Chung et al., 1970; Zucker, 1974; Raymond and Lettvin, 1978), and that these mechanisms might be necessary to guarantee the coherent behavior of large populations of neurons (Lüscher et al., 1979, 1982).

Terminal arborizations in the mammalian central nervous system are in fact of great complexity, with large numbers of successive branch points, boutons en passant and terminal boutons. All these inhomogeneities could influence impulse propagation and activation of presynaptic terminals. Synaptic boutons residing on extremely small terminal branches represent an especially large electrical load to the propagated action potential. Failures

Address correspondence to Professor H.-R. Lüscher, Department of Physiology, University of Bern, Bühlplatz 5, CH-3012 Bern, Switzerland.

of propagation of action potentials at branch points and reflections at synaptic endings might give rise to complex patterns of synapse activation. Unfortunately, these structures are not accessible to intracellular recordings and can not be investigated directly. Theoretical analyses of the effect of branch length and synaptic boutons on impulse propagation in terminal arborizations have been lacking until now. In this paper we present the results of a computer simulation study on the propagation of single action potentials in bifurcating axons carrying synaptic boutons on short collaterals. The membrane model used in this simulation study was derived from Hodgkin and Huxley (1952). Because no experimental data are available on membrane properties of central terminations, uniform membrane properties were assumed and the accumulation of periaxonal potassium was not taken into account. Because repetitive stimulation is not considered in this study, and temperature was kept constant at 22°C for all simulations, the only parameter affecting impulse propagation was the geometry of the structure simulated.

It will be shown that synaptic boutons residing on short branches might be activated without being reached directly by an action potential. In addition, two critical branch lengths exist between which failure to activate the synaptic bouton occurs; branches with lengths outside this critical range lead to successful activation of the bouton. It will further be shown that propagation through critical branch points can be enhanced by inserting a bouton of critical size at the bifurcation. Differential activation of the two synaptic boutons residing on short collaterals of a bifurcating axon can also be observed.

MATERIALS AND METHODS

Simulation

Our approach to the simulation of the propagation of action potentials in the terminal branching of an axon is based on the work of Segev et al. (1985) and Bunow et al. (1985), who described the application of a general purpose electrical circuit simulation program called SPICE (Vladimirescu et al., 1981) to the modeling of the electrical behavior of neurons with arbitrarily complex dendritic trees. Because we are interested in using SPICE for simulating spike propagation in morphologically complex terminal arborizations we developed a software package called SPAX which automatically generates the SPICE code from a simple list describing the architecture of the branching structure. Thus, we could avoid the tedious work of entering the SPICE code for a complex multisegment structure from a computer terminal. A short description of SPAX will be given in the Appendix.

Validation of the model

The performance of SPICE has been tested extensively for passive dendritic trees (Segev et al., 1985) by comparing the SPICE results to analytical solutions derived by Rall and Rinzel (Rall, 1959; Rinzel and Rall, 1974). Similar tests were done by Bunow et al. (1985) for Hodgkin-Huxley axons of simple geometry. For several critical cases they demonstrated that SPICE approximated the correct solution to the equations for the propagating action potential extremely well. One such critical test is the behavior of the propagating action potential through a branch point with a geometrical ratio (GR) larger than unity (Goldstein and Rall, 1974). The geometrical ratio is defined as $GR = \Sigma_j d_j^{3/2}/d_a^{3/2}$, where d_j is the diameter of the jth daughter branch, the summation is over all these daughter branches, and d_a is the diameter of the parent branch. If GR is increased beyond a critical value, the action potential does not propagate into the daughter branches. The critical value of GR for propagation failure is temperature sensitive. At lower temperatures the critical value of GR is higher than at higher temperatures (Westerfield et al., 1978). Like Bunow et al. (1985), we have studied the behavior of the propagating action potential through branch points of increasing GR at different temperatures in order to validate the performance of our SPICE version and of SPAX. Fig. 1 *A* illustrates the simulation of the propagating spike in axon arborizations at a temperature of 16.5°C. The axon divides into 5, 12, 14, and 17 daughter branches of diameter equal to that of the parent axon. Therefore, GR is equal to the number of daughter branches.

As the action potential approaches the branch point the peak amplitude falls and the conduction velocity becomes slower. A second peak develops in the falling phase of the action potential. These features get more pronounced the larger GR gets. At $GR = 17$ (Fig. 1 *A d*) the action potential fails to propagate past the branch point. It is important to note that the action potential fails while approaching the branch point. At the branch point itself (*point* 3 in Fig. 1 *A d*) the amplitude of the failing action potential is very small and there is virtually no passive spread of the potential into the daughter branches. In Fig. 1 *A b* and Fig. 1 *A c* a decremental reverse conduction (*arrows*) can be observed. If different GRs were used, this decremental conduction might be converted to nondecremental reverse conduction as demonstrated by Goldstein and Rall (1974) and Bunow et al. (1985).

In Fig. 1 *B* similar branching schemes with $GR = 3$, 5, 7, and 9 are simulated at a higher temperature (22.5°C). The basic features of the propagation of the action potential through the branch point are very similar to those observed in Fig. 1 *A*, but as expected, propagation failure occurs at $GR = 9$, a lower value than for $T = 16.5$°C. The simulation shows smooth conduction through a bifurcation with a $GR = 1.0$ and long branches compared to the resting length constant.

Because this and the companion paper (Lüscher and Shiner, 1990) deal exclusively with action potential propagation into axon terminations with sealed ends, we have simulated the changes in shape and velocity of the action potential as it approaches a sealed boundary. The result of such a simulation with SPAX is illustrated in Fig. 2. As in the analytical results of a similar computation given by Goldstein and Rall (1974), both the amplitude and conduction velocity increase as the action potential approaches the sealed axon termination.

In agreement with Bunow et al. (1985) we conclude that SPICE correctly solves the equations for propagating action potentials with sufficient accuracy in several critical cases. Therefore, we expect that the solutions obtained from our program for other, morphologically far more complex, structures are likely to be correct.

RESULTS

Terminal boutons on very short collaterals represent a large electrical load for an approaching action potential, the load depending on the branch length. In this case propagation past a bifurcation does not depend only on GR, because GR is defined for long branches with uniform membrane and cable properties (Rall 1959;

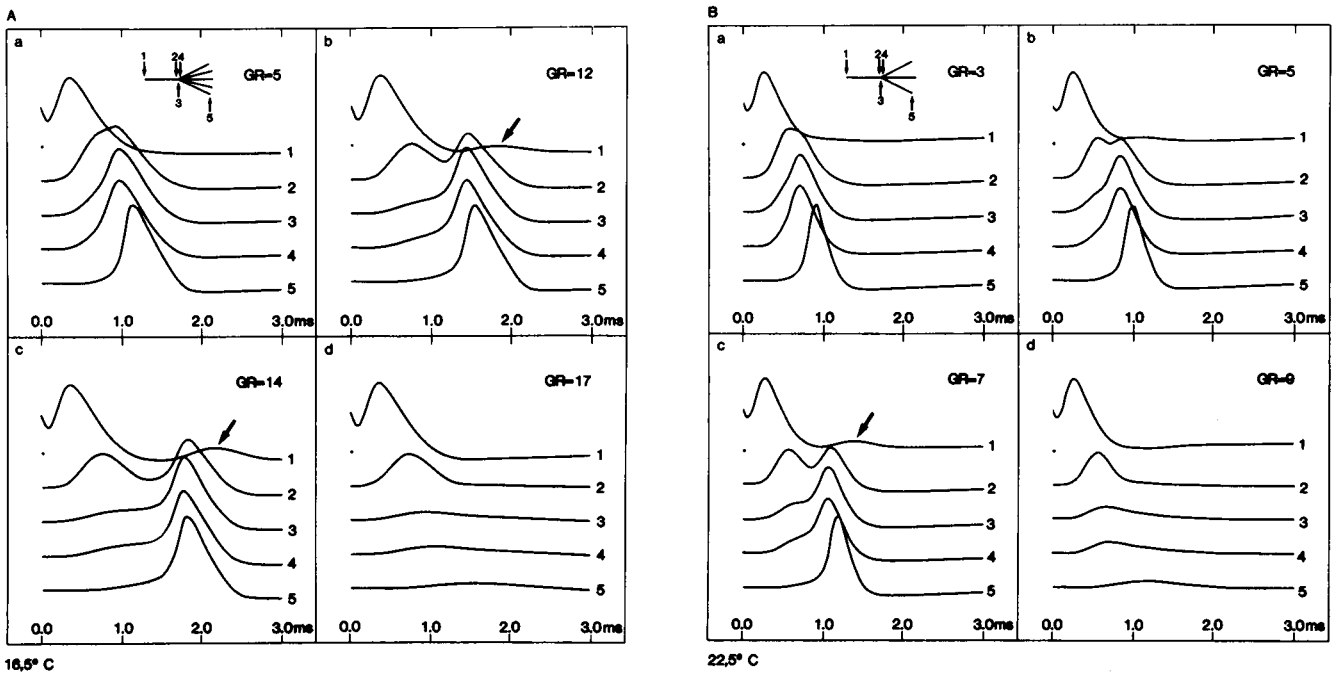

FIGURE 1 Simulation of action potential propagation through axon branch points of different geometrical ratio at temperatures of 16.5°C (*A*) and 22.5°C (*B*). All branches are of equal diameter. Therefore, the geometrical ratio (*GR*) is equal to the number of daughter branches. In each case, the sequence of recording sites is illustrated in the branching scheme in the two upper left panels. The action potential is initiated at recording site 1, the first compartment of the parent axon. Recording sites 2, 3, and 4 are the last compartment just ahead of the branch point, the branch point itself, and the first compartment just after the branch point, respectively. Recording site 5 is one of the last compartments of the daughter branches. At low temperature, 16.5°C (*A*), the action potential fails to propagate past the branch point at $GR = 17$. At the higher temperature, 22.5°C (*B*), the action potential fails at $GR = 9$. The arrows point to decremental reverse conduction due to reflection at the branch point.

Goldstein and Rall, 1974). We first studied action potential propagation through a bifurcating terminal branch with one short collateral of constant length and a second collateral of increasing length.

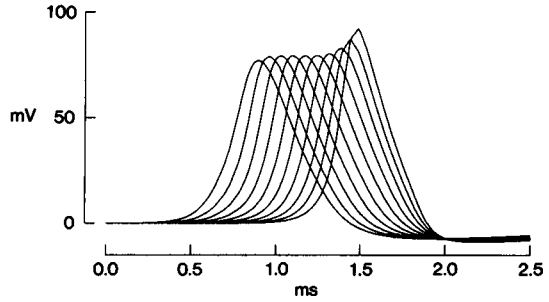

FIGURE 2 Simulation of a propagated action potential in a homogeneous axon as it approaches a sealed end. The action potential is shown at the last 10 compartments of the axon. The length of the compartments was two-tenths of the resting electrical length constant, and the integration interval was 0.01 ms. Both amplitude and conduction velocity increase as the action potential approaches the sealed axon termination.

Influence of branch length

Fig. 3 *A–D* illustrate the propagation of an action potential along the mother branch as it approaches the bifurcation and its propagation or failure to propagate into the daughter branches. The diameters of unmyelinated terminal branches in the mammalian central nervous system are extremely small (0.4–0.1 μm; Fyffe and Light, 1984). In comparison, the synaptic boutons they carry are very large (4–5 μm along their long axis; Fyffe and Light, 1984). The diameter of the axon we used for simulation was 0.1 μm. The length of collateral *b* was 19 μm and was kept constant. The diameter of bouton *B* was 4 μm, and its length 6 μm. The length of collateral *a* varied between 2.5 and 100 μm. The diameter of bouton *A* was also 4 μm, and its length was 5 μm. The diameters of the daughter branches were the same as that of the mother branch. For long collaterals *GR* would therefore be two. The calculated resting length constant for this axon is 71.5 μm, which is very long compared to the collateral length. These geometrical values are used for illustrative purposes. Other values might lead to quantitatively different results because, as will be shown later, small differences in

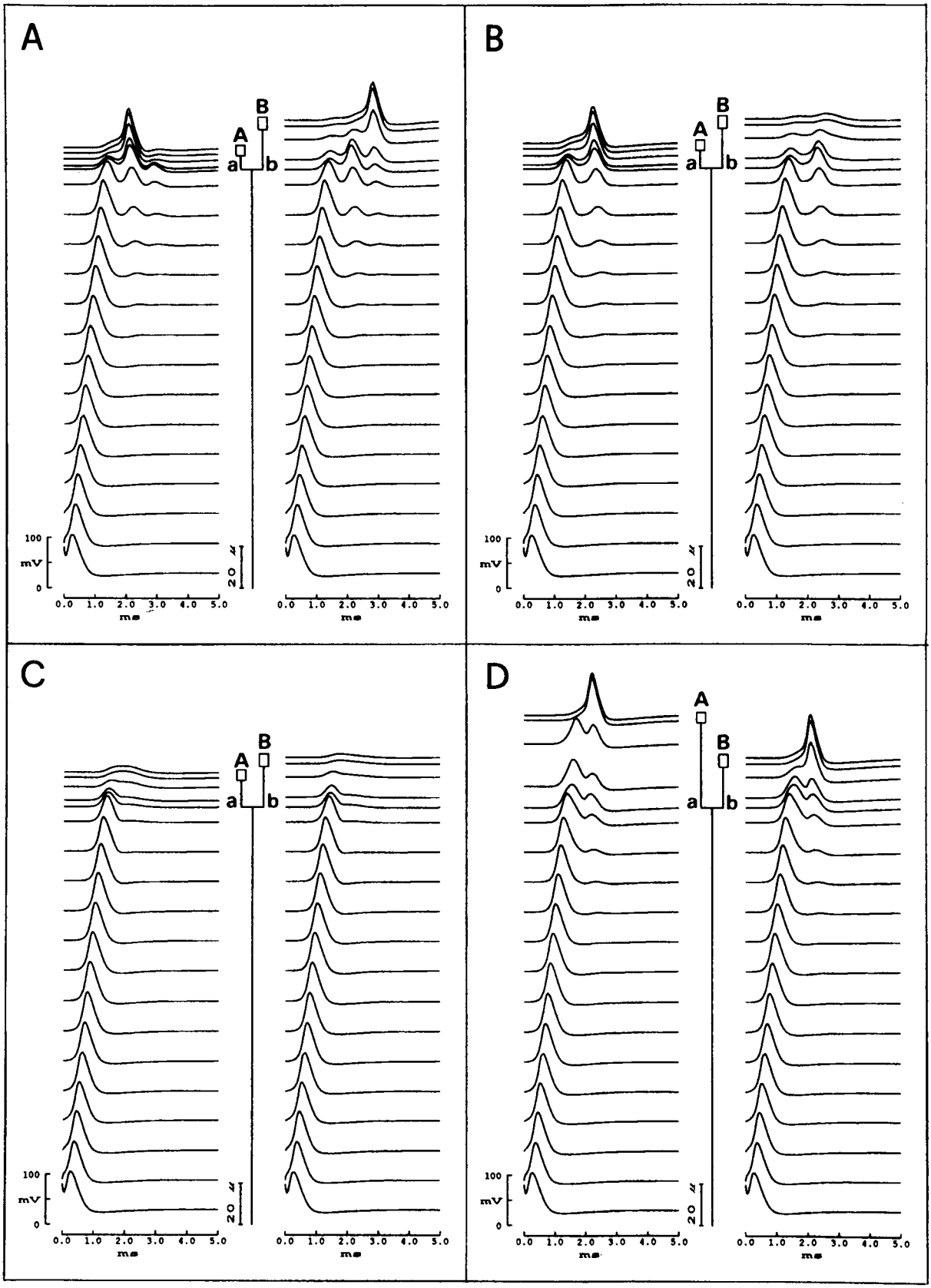
A
B
C
D
A
B
a
b
100
mV
0
20 μ
0.0 1.0 2.0 3.0 4.0 5.0
ms

geometry may lead to different propagation behavior of the action potential. In Fig. 3 *A* the action potential was initiated as the beginning of the axon by displacing the membrane potential to 50 mV (V_{rest} = 0 mV). The spike propagates with a constant velocity of 0.22 m/s along the axon. As it approaches the branch point it slows down and its amplitude decreases. It does not actively propagate either into branch *a*, which was 6.5 μm long, or into branch *b*, which was 19.0 μm long. Instead, the current which passively spreads into bouton *A* depolarizes bouton *A* above threshold initiating an action potential which propagates back into the main axon where it dies out during the refractory period of the approaching action potential. The electrotonic spread of this reverse conducted action potential is sufficient to depolarize bouton *B* above threshold, initiating a second action potential which again leads to a decremental reverse conduction. It is the reflection of the passive spread of the current at the sealed end of the bouton which increases the membrane potential above threshold, thus, initiating an action potential in the bouton. The sequence of events can be summarized as follows: (*a*) the action potential fails to propagate actively beyond the branch point because of impedance mismatch; (*b*) the electrotonic current spread along the short collateral initiates a new action potential in bouton *A* but not in bouton *B*, which resides on a longer collateral; (*c*) the new action potential propagates antidromically to the branch point where it fails again; (*d*) the electrotonic spread of the failing action potential initiates a new action potential in bouton *B*, which again is propagated back to the branch point where it fails again. It cannot activate bouton *A* a second time because bouton *A* is still in the relative refractory state. A potential continued sequential activation of the two boutons is thus terminated. Because the synaptic boutons are not directly depolarized by the approaching action potential the delay for activating the synaptic boutons is long with an even longer temporal dispersion between the two terminal boutons.

Fig. 3 *B* illustrates a similar simulation. The length of collateral *a* was increased by 3 to 9.5 μm. A similar sequence of events can be seen. The approaching action potential fails at the branch point. The electrotonic spread of the potential along branch *a* is still able to evoke an action potential in bouton *A* but not in bouton *B*. This potential propagates back to the branch point where it fails. Because the amplitude of the reverse conducted action potential is slightly smaller at the branch point than in the case described in Fig. 3 *A*, its passive conduction along branch *b* is insufficient to generate an action potential in bouton *B*, leading to differential activation of the two terminal boutons.

If collateral *a* is lengthened by an additional 2.5 μm to a total length of 12.0 μm both boutons *A* and *B* fail to be activated. This is illustrated in Fig. 3 *C*. In this case the synaptic boutons are still close enough to the branch point to represent a large electrical load to the approaching action potential, which leads to propagation failure. On the other hand, they are too far away to be depolarized above threshold by electrotonically propagated potential. It is worth noting here that the action potential fails while approaching the critical branch point. At the bifurcation itself the amplitude of the action potential is less than one third of its initial value. The additional rapid decremental decay of the small action potential along the short collaterals leads to only a very small depolarization of the synaptic boutons, which would probably not be sufficient to trigger transmitter release.

If the length of collateral *a* is further increased as illustrated in Fig. 3 *D* the action potential propagates actively past the branch point into both collaterals. Because *GR* is larger than unity, propagation is delayed at the branch point as expected. In addition a decremental reverse conduction at the branch point can be observed.

Fig. 4 summarizes the results of 17 different simulations (including the ones illustrated in Fig. 3). The length of collateral *b* was kept constant whereas the length of branch *a* was increased from 2.5 to 100 μm. It should be remembered that these are short collaterals if compared to the resting length constant of 71.5 μm. If activation of a bouton by an action potential or failure of its activation is regarded as a logic state + or −, respectively, a logic diagram of activation of the terminal boutons can be compiled and related to branch length *a*. Such a logic diagram is illustrated in Fig. 4. If branch *a* is short, both boutons *A* and *B* are on. Because the large electrical loads of the two boutons are very close to the branch point the action potential fails to propagate past the branch point. But because bouton *A* is so close to the branch point the passive spread of the potential is sufficient to evoke an action potential in *A*. *B* is activated by the action potential conducted back from branch *a* (see Fig. 3 *A*). If bouton *A* is moved away from the branch point the electrical load it

FIGURE 3 Action potential propagation along a bifurcating axon with short collaterals carrying synaptic boutons. A drawing of the axon structure is given in the middle of each panel. On the left side in each panel, the action potentials are illustrated for each compartment of the structure as it propagates along the main axon and into collateral *a*. On the right side in each panel, the action potentials are illustrated for each compartment of the structure as it propagates along the main axon and into collateral *b*. The action potential is always initiated at the first compartment of the main axon. The length of collateral *b* is constant (19.0 μm). The length of collateral *a* is 6.5 μm (*A*), 9.5 μm (*B*), 12.0 μm (*C*), and 40.0 μm (*D*). The activation pattern of synapse *A* and *B* is different for different lengths of collateral *a*. Further explanation in the text.

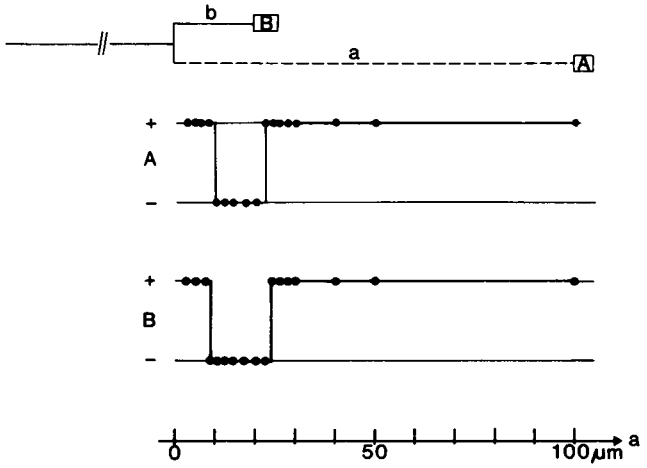

FIGURE 4. Logic diagram of synapse activation for a bifurcating terminal arborization with one collateral of constant length (b = 19.0 μm) and one collateral (a) of increasing length, ranging from 2.5 to 100.0 μm. All the other dimensions are the same as used in Fig. 3. The + sign indicates that the synapse develops an action potential, whereas the − sign indicates a silent synapse. There exists a critical region of length a for which both synapses remain silent. At the onset and at the end of this critical region differential activation of the two synapses can be observed.

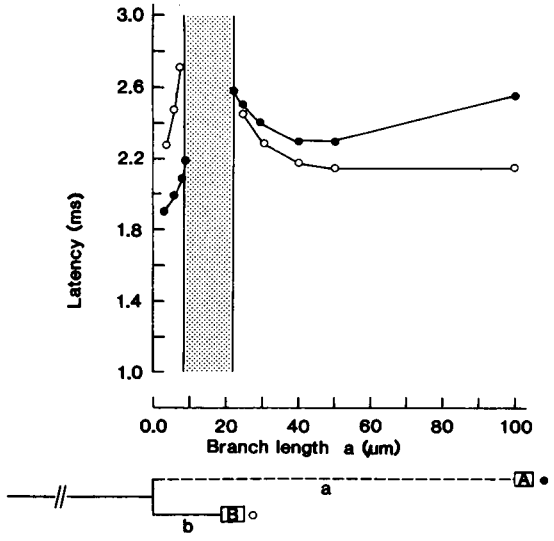

FIGURE 5 Plot of collateral length a against latency of synapse activation. Branch length b is constant (19.0 μ). All the other dimensions are identical to the dimensions used in Fig. 4. Open symbols indicate latency for synapse B. Solid symbols indicate latency for synapse A. Stippled area indicates the region of branch length a for which synapse A and B remain silent. There is a steep increase in latency before the critical range for collateral length a resulting in failure of synapse activation.

represents to the branch point decreases, but is still large enough to cause the action potential to fail. Because the passively propagated potential decays below a critical value along the longer branch a, no action potential is generated in bouton A. At a critical length only bouton A is activated (see also Fig. 3 B). If the length of branch a increases beyond a critical value, the electrical load it represents to the branch point falls below the critical value for propagation failure. The action potential propagates beyond the branch point reaching both bouton A and B. There is again a critical length for which differential activation of the two synaptic boutons can be observed.

This series of simulations clearly indicates the existence of a critical branch length which leads to failure of activation of the terminal bouton. It also demonstrates that GR is not a useful indicator for the safety factor of spike propagation if the daughter branches are short compared to the passive electrotonic length of the axon.

The delay and degree of synchronization of the activation of the synaptic boutons are important for the activation of the postsynaptic neuron. In Fig. 5 the latency of activation of the terminal boutons is plotted against branch length a. Latency is defined as the difference between the time of initiation of the action potential at the initial segment of the parent axon and the time when the action potential in bouton A or B reached 50.0 mV. As long as branch a is short, the latency for activating bouton A is much shorter than for bouton B and increases for both boutons with increasing length of branch a up to the point where first bouton B and later bouton A fail to evoke an action potential. The steep increase in latency is explained by an increased local response time when the depolarizing current comes close to threshold.

If the length of branch a is increased beyond the critical length, the branch point starts to conduct and the action potential propagates actively into the terminals. Because this happens when a is longer than b, the latency for activating bouton B is shorter than for activating bouton A. The farther away the electrical load of bouton a moves from the branch point, the shorter the propagation delay at the branch point. This leads to a decrease in latency up to the point where the linear increase in conduction time with increasing length of branch a leads to a linear increase in latency for activating bouton A. Because the length of b remains constant the latency for activating bouton B remains constant as soon as the electrical load represented by bouton A is too far away from the branch point to affect its load at the branch point to a significant degree.

Influence of branch point swellings

Within terminal arborizations, short collaterals quite often arise from axon swellings which cannot be distin-

guished from synaptic boutons by light microscopy (Brown and Fyffe, 1978). In cultured rat spinal cord slices we have often observed a similar short but rapid flaring of the axon at branch points (unpublished observation). In view of the observations of the previous section this axon specialization might improve the safety factor for impulse propagation by increasing the current density in the short daughter branches which carry the synaptic boutons representing the large electrical load.

Fig. 6 *A* and *B* illustrate the simulation of action potential propagation through a structure identical to the one of Fig. 3 *C* except that it has an axon swelling at the branch point. Without this branch point swelling neither bouton *A* nor *B* are activated by an action potential (compare Fig. 3 *C*). With the axon swelling both bouton *A* and *B* are activated with short latency (Fig. 6 *A*). The conduction velocity of the action potential and its amplitude decrease while approaching the swelling as expected for a steep increase in axon diameter.

With a short delay the swelling develops an action potential of normal amplitude. This action potential develops enough current to excite the two daughter branches. Each branch together with its attached synaptic boutons is excited almost simultaneously along its entire length. In this example the swelling at the branch point acts as a booster to improve invasion of the action potential into the terminal arborization.

Small swellings decrease the safety factor as illustrated in Fig. 7. It illustrates the structure which, without the small axon swelling at the branch point leads to differential activation of terminal boutons *A* (see Fig. 3 *B*). Adding the small swelling leads to complete propagation failure.

If the swelling increases beyond a critical size the

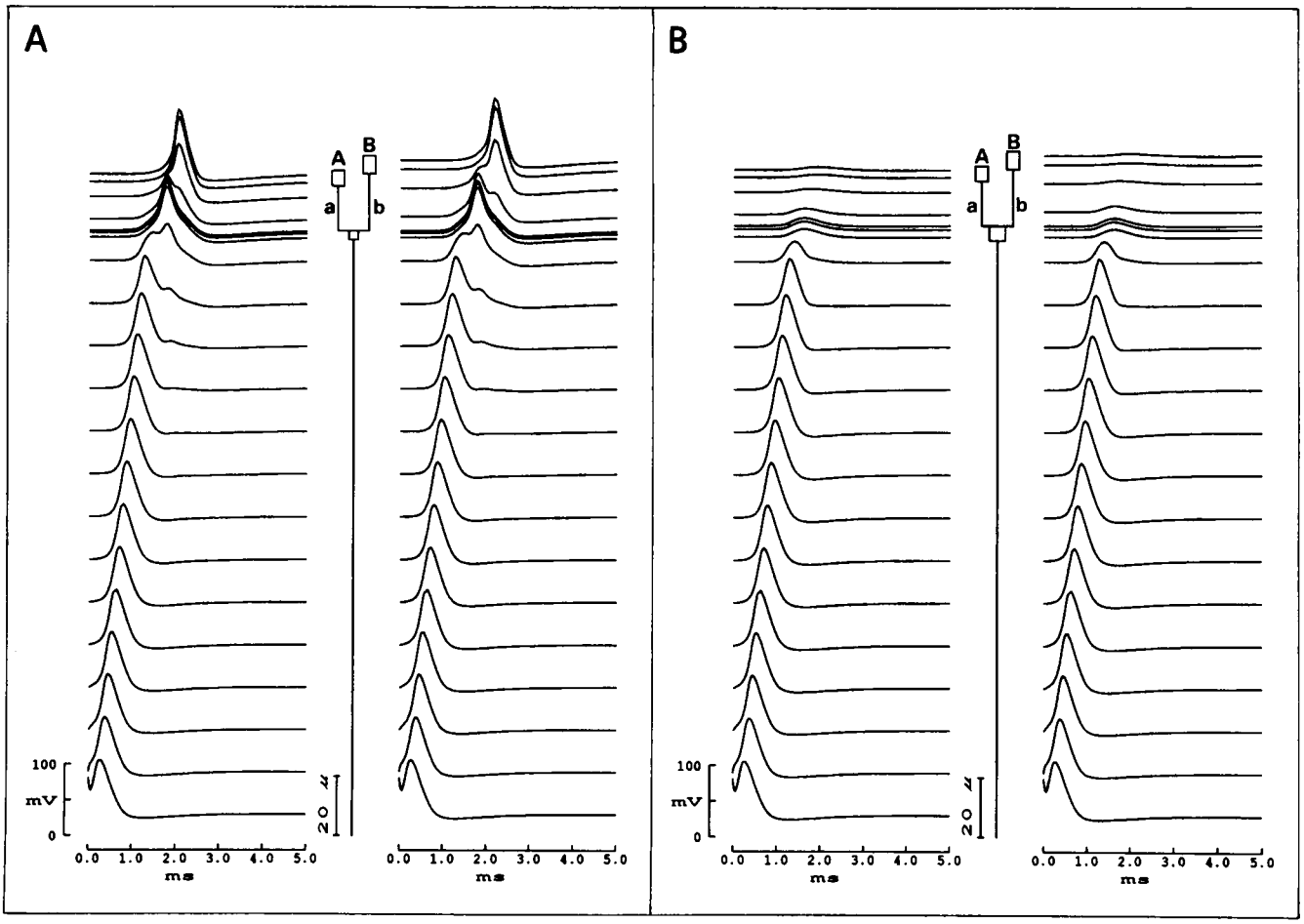

FIGURE 6 Simulation of action potential propagation along the same structure as illustrated in Fig. 3 *C*, but with axon swellings introduced at the branch point (*A*, diameter and length = 3.0 μm; *B*, diameter and length = 5.0 μm). Without the swellings both synapses *A* and *B* remain silent (compare Fig. 3 *C*). The smaller swelling acts as a booster leading to the activation of both synapses *A* and *B* with short latency. The larger swelling leads to complete propagation failure.

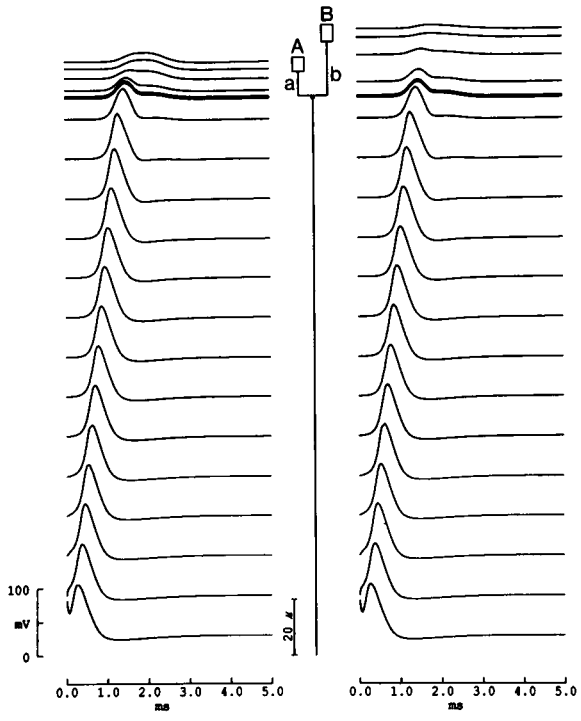

FIGURE 7 Simulation of action potential propagation along the same structure as in Fig. 3 *B*, but with a very small axon swelling (diameter 1.0 μm, length 1.0 μm) at the branch point. This small axon swelling decreases the safety factor, resulting in silent synapses. Without the swelling, synapse *A* would be activated (compare with Fig. 3 *B*).

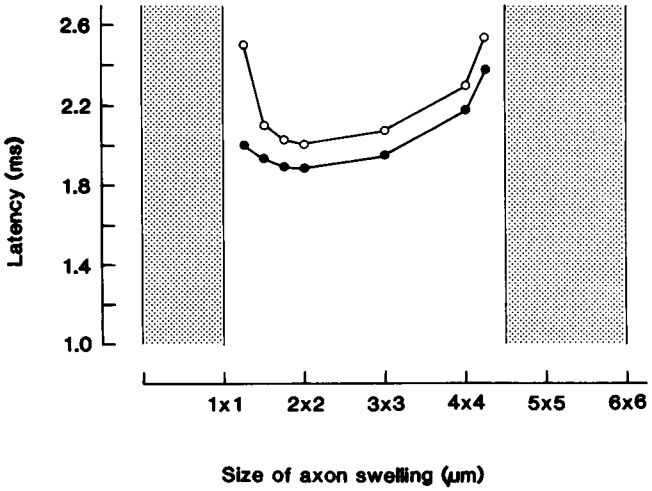

FIGURE 8 Plot of size of axon swelling at the branch point against latency of synapse activation. Except for the axon swelling, same structure as in Fig. 3 *C*. Open symbols indicate latency for activating synapse *B*. Solid symbols indicate latency for activating synapse *A*. The numbers on the abscissa represent bouton diameter times bouton length. The stippled areas indicate the range of bouton sizes at the branch point for which complete failure occur. The bouton has to have a minimal size to act as an effective booster. An optimal bouton size exists for minimal latency of synapse activation. Above a certain bouton size, the safety factor decreases and propagation failure is eventually induced.

action potential fails again while approaching the branch point swelling (Fig. 6 *B*). In this case the three boutons together represent too big an electrical load to allow the action potential to propagate.

In Fig. 8 the spike latencies in synapse *A* (.) and *B* (o) are plotted against the size of the branch point swelling. Swellings smaller than 1.0 × 1.0 μm are insufficient to boost the action potential into the daughter branches, whereas swellings larger than 4.5 × 4.5 μm lead to propagation failure ahead of the booster due to the increased electrical load (*stippled area*). There exists an optimal size for the booster where it activates the two terminal boutons with the shortest latency.

DISCUSSION

The present simulations demonstrate that synaptic swellings near bifurcations have a profound effect on the safety factor for impulse propagation due to their added electrical load. If the boutons are close enough to the bifurcation, the electronic spread of the current which is reflected at the sealed end of the terminal boutons might depolarize the terminal above threshold, thus, initiating an action potential. In this case, even though the action potential fails to propagate beyond the branch point, the synaptic bouton close to the branch point can be activated and release transmitter. On the other hand, if the synaptic bouton resides on a longer collateral, the electrical load it represents to the branch point might still induce conduction failure, but the electrotonic decay of the potential progresses too far for the potential to evoke an action potential in the synaptic terminal. If the two collaterals have different lengths differential activation of the synaptic boutons may occur even though the action potential fails to propagate past the branch point. Only if the boutons are far from the branch point does their load not affect conduction any more. From this discussion it is evident that the geometric ratio alone does not determine the safety factor for impulse propagation in terminal arborizations with short branches.

It might be argued that failure of an action potential to invade a terminal arborization should have no effect on transmitter release because the electrotonic spread of the potential would depolarize the terminals sufficiently to trigger transmitter release provided that the space constant is long compared to the lengths of the collaterals. This would be a misconception of the branch point failure mechanism, however, because the action potential does not fail at the branch point proper, but rather declines

progressively while approaching the branch point. In addition, the large load represented by the synaptic swelling leads to a very steep decay of what is left of the action potential at the branch point. On the other hand, because the terminal boutons represent an open circuit sealed end structure, small currents entering the swelling might depolarize it above threshold, initiating an action potential without being actively invaded by the propagated action potential. This spike initiation would guarantee proper activation of the calcium channels in the terminals. It has been proposed that L-type calcium channels regulate transmitter release from rat and chick sensory ganglia (Perney et al., 1986). In other systems the N-type calcium channels may play a dominant role in controlling transmitter release (Hirning et al., 1988). These channels are activated at membrane potentials more positive than -10 and -20 mV, respectively. This is certainly above the firing threshold for initiating an action potential. Passively conducted potentials which are too small to evoke an action potential in the terminal will also not be able to activate the calcium channels and, thus, no transmitter would be released.

The above discussion is based on the assumption that the membrane of the synaptic endings has a sufficient density of Na^+ channels to carry an action potential. It is certainly a simplification to assume uniform membrane properties throughout the whole terminal arborization. Mallart and his collaborators identified Na^+, Ca^{2+} and two different types of K^+ currents in the motor nerve endings of the mouse (Brigant and Mallart, 1982; Mallart, 1985). In the motor nerve terminals of the lizard, Na^+ channels provide the major ionic current pathway in the heminode, whereas K^+ channels are the major pathway in the terminal boutons and branches, but there is some overlap in their distribution (Lindgren and Moore, 1989). No similar information is available for terminal arborizations in the central nervous system.

Our simulations suggest that there is a critical range of branch lengths where activation of the attached terminal boutons fails to occur. Below this critical range the synaptic bouton can be activated through electrotonic current spread; above this critical range the bouton is actively invaded by the propagated action potential. This critical range is of course very much dependent on the assumptions made about the distribution and density of the voltage-dependent ionic channels as well as on the detailed dimensions of the structure. It is therefore impossible to examine reconstructed terminal arborizations to verify whether or not such critical ranges of collateral lengths are avoided by nature. On the other hand, our simulations also suggest that branch point swellings can restore the activation of synaptic boutons located at collaterals with lengths in the critical range. To function as an effective booster these swellings must lie within a certain range of sizes. Below and above this range the safety factor drops below the critical value for impulse propagation. Moreover there is an optimal size of the booster for the shortest delay in activating the synaptic bouton. Brown and Fyffe (1978; 1979) have published a number of reconstructed terminal arborizations from Ia and Ib afferents intracellularly labeled with HRP. Some of these terminal arborizations show boutons at branch points having dimensions of 1.5×2.5 μm up to 2.0×6.0 μm. These dimensions are well within the range of the effective boosters. With light microscopy it cannot be decided whether or not these swellings are presynaptic structures capable of releasing transmitter. They are usually counted as such if they are in close apposition to postsynaptic elements (Brown and Fyffe, 1978; Burket et al., 1979). If in fact these branch point swellings represent synaptic boutons they may serve a double function; they may also function as boosters to improve the safety factor for action potential propagation.

Ultrastructural studies of group Ia afferent fibers in the cat spinal cord have revealed that preterminal branches are myelinated, whereas axonal segments linking en passant synapses are usually only very lightly myelinated or unmyelinated (Fyffe and Light, 1984). On the assumption that the diameter of the axon does not change at the transition from a myelinated part to the unmyelinated terminal region, which may not be the case, this transition would reduce the safety factor for impulse propagation considerably, because the current generated in the final node would not be sufficient to depolarize the large unmyelinated terminal arborization. The distance between the nodes must be shortened near the nerve endings to guarantee impulse propagation into the terminal arborization. This conclusion was drawn by Revenko et al. (1973) and Waxman and Wood (1984) from simulation studies. Similarly, Waxman and Brill (1978) demonstrated that impulse conduction through demyelinated regions is facilitated by reducing the internodal length ahead of these regions. In fact, Quick et al. (1979) and Lindgren and Moore (1989) found that the internodal length gradually decreases near the motor nerve endings. Similarly, Ito and Takahashi (1960) have demonstrated in dorsal root ganglia a decrease in internodal length just before the bifurcation. Closely spaced nodes of Ranvier have also been observed in the mammalian brain (Waxman and Melker, 1971; Deschênes and Landry, 1980). The safety factor, however, is not only determined by internodal length but also by nodal area. Large nodes at branch points of otherwise low security could compensate for the large impedance mismatch, as our simulations show. Similarly, the properties of the heminode at the transition from the myelinated to the unmyelinated part of the axon might determine the invasion characteristics of the terminal branches (Waxman and Wood, 1984).

The present simulations demonstrate that single action potentials can activate terminal boutons by two different mechanisms and that activation of synaptic boutons may be complex. The reflection of the action potential at branch points or terminal boutons leading to decremental reverse conduction would interact in a complex manner with the ensuing impulse in a train of action potentials. Depending on the interpulse interval, facilitation or depression of synapse activation could be expected. It has been shown that potassium buildup in the periaxonal space during repetitive activation of an axon contributes to the development of conduction failure (Grossman et al., 1979*a*, *b*; Smith, 1983*a*). This mechanism, working on a slow time-scale, would interact with the structural features of the terminal arborizations and the refractory and supernormal periods of the axon membrane. Without even taking into account the periaxonal potassium buildup, it has been shown that changes in the membrane excitability and propagation delays caused by geometric factors lead to complex asymmetrical patterns of propagation into the daughter branches which depend on the impulse frequency in the parent axon (Stockbridge, 1988*b*; Stockbridge and Stockbridge, 1988).

To predict the impulse propagation pattern and activation of synaptic boutons in a simple terminal arborization, detailed knowledge of the structure of the arborization and membrane properties would be needed. In more complex arborizations consisting of several branch points, boutons en passant and terminal boutons, the activation pattern or synaptic boutons may no longer be predictable. Small changes in membrane excitability after an impulse might be amplified as the action potentials invade the terminal arborization leading to irregular activation of the synaptic endings. Because terminal arborizations show an enormous structural variability, they might exhibit different activation patterns at their terminals. It is not apparent whether and, if so, how the nervous system takes advantage of this enormous potential for presynaptic information processing. It remains to be elucidated whether the structure of terminal arborizations in the central nervous system is optimized to guarantee propagation of the nervous impulse to the destination given by the structure of the axon arborizations, or whether failure of synapse activation represents a basic design principle enhancing the capabilities of the central nervous system for information processing.

APPENDIX

SPAX is a FORTRAN program which calls SPICE9 (Version 2G.6) as a subroutine. In addition, SPAX compresses the output from SPICE and generates a display file for a 4010 graphics terminal (Tektronix Inc., Beaverton, OR). The time course of the membrane potentials of all or selected compartments and branch points as well as the various currents can be selected for display.

SPAX takes its input from a file whose main body is a list of the axon segments in the terminal branching along with their properties: dimensions, whether excitable or passive, and connections to other segments. A segment is defined as an interconnected cylindrical stretch of axon of known length and diameter with uniform membrane properties. A program line describing a segment has the following form: *oo-bbb-sssT d l bp nd bd*, where *oo* the order, *bbb* is the branch and *sss* the segment of the branching. *T* specifies the type of the segment (P = passive, H = active, nonmyelinated). *d* is the diameter of the segment, and *l* its length. *bp* is the branch of order *oo*-1 to which the first segment of order and branch *oo-bbb* is connected proximally. *bp* is input only when *sss* = 001 and *oo-bbb* ≠ 00-001). *nd* and *bd* are the number of branches and the first branch, respectively, of order *oo* + 1 to which the last segment of order and branch *oo-bbb* is connected distally. *nd* and *bd* are input only for the last segment of order and branch *oo-bbb*. For a terminal segment *bd* = *nd* = 0. The process used to transform the architecture of a complex arborization into the input list of SPAX is illustrated in Fig. 9.

Fig. 9 *A* shows a hypothetical random arborization with synaptic terminal boutons and boutons en passant. The branching scheme is not

A

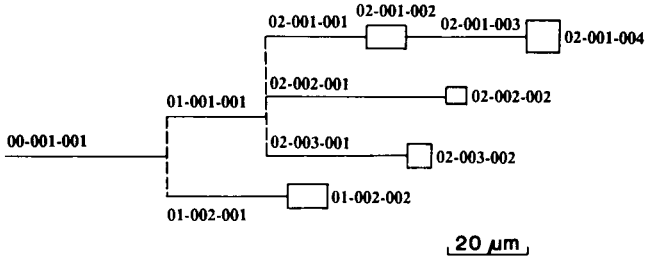

B

```
TITLE ARBOR
SQUID
TEMP 22.0
00-001-001H   0.3   40.0   2   1
01-001-001H   0.2   25.0   1   3   1
01-002-001H   0.2   30.0   1
01-002-002H   6.0   10.0   0   0
02-001-001H   0.2   25.0   1
02-001-002H   6.0   10.0
02-001-003H   0.1   30.0
02-001-004H   8.0    8.0   0   0
02-002-001H   0.2   45.0   1
02-002-002H   4.0    5.0   0   0
02-003-001H   0.2   35.0   1
02-003-002H   6.0    6.0   0   0
SEGEND
START IC 50.0
TIMING 0.005 0.00001
OUTPUT ALLI
ENDOUT
```

FIGURE 9 (*A*) Coding of a hypothetical branching scheme. (*B*) Entire listing of the SPAX-Program to calculate the propagation of an action potential along the structure illustrated in *A*. Further explanation in the text.

binary. The stated rules above are applied to generate the lines (printed bold in Fig. 9 *B*) which specify the segments of the structure. Because SPICE can only treat circuits with discrete elements, each axon segment must be divided into compartments small enough that the simulation yields a good approximation to the continuous axon. SPAX automatically divides the segments into compartments with an electrotonic length $X = 0.2\lambda$ (λ = resting length constant). It was shown (Segev et al., 1985) that for passive segments SPICE yields very accurate results with a maximum electrical length criterion for each compartment of 0.2 λ, when compared with an analytical result. If a segment was $< 0.2\lambda$ it was always split into two compartments of equal size, as in the work of Bunow et al. (1985).

In addition to the lines coding the branching structure, the temperature and the name for the default parameters must be specified. In this study all simulations were run at 22°C. SQUID means that the standard Hodgkin-Huxley parameters (Hodgkin and Huxley, 1952) are used as listed in Table 1.

Information on how the action potential is to be initiated at the initial compartment of the branching scheme is input in the line beginning with 'START'. A single action potential can be initiated by setting the initial condition of the membrane potential above threshold. As an alternative the initial compartment can be stimulated with repetitive current pulses. Information on the duration of simulation and the time step for integration are given in the third to last line. The desired output is specified in the second to last line.

All simulations were carried out on either a μVAX II, μVAX 3500 or a VAX 6000-310 running under VMS. The simulations took approximately three times longer on the μVAX II than on the other two machines. In principle SPAX allows structures of up to 99 orders, 999 branches per order, 999 segments per branch, and 99 compartments per segment. In practice, however, much smaller numbers were used to reduce computation time. As a guideline, structures with 30, 65, 75, and 90 "active" Hudgkin-Huxley compartments used, depending on the specified temperature, ~2.5, 4.3, 5.5, and 7.1 h CPU-time on a μVAX II. Passive membrane compartments use much less time for simulation. We found that slow execution is the only serious disadvantage of SPICE for this kind of work. A CRAY version of SPAX is in preparation, and preliminary results indicate that the simulations will run only four to five times faster on a CRAY X-MP as on the VAX 6000-310.

We are grateful to the Informatik Dienste and the Institut für Informatik und angewandte Mathematik of the Univeristy of Berne for the use of their computing facilities. We wish to thank Dr. H. P. Clamann for reading the manuscript.

The work was supported by the Swiss National Science Foundation (Grant No. 3.265-0.85) and the Swiss Multiple Sclerosis Society.

TABLE 1 Default parameters for H-H equations

R_m* = $1.0 \cdot 10^{12}\ \Omega\mu m^2$	$= 10^4\ \Omega cm^2$
$R_i = 7.0 \cdot 10^5\ \Omega\mu m$	$= 70\ \Omega cm$
$C_m = 10^{-14}\ F/\mu m^2$	$= 1.0\ \mu F/cm^2$
$g_{Na} = 1.2 \cdot 10^{-9}\ mho/\mu m^2$	$= 1.2 \cdot 10^{-1}\ S/cm^2$
$g_K = 3.6 \cdot 10^{-10}\ mho/\mu m^2$	$= 3.6 \cdot 10^{-2}\ S/cm^2$
$g_l = 3.0 \cdot 10^{-12}\ mho/\mu m^2$	$= 3.0 \cdot 10^{-4}\ S/cm^2$
$V_{Na} = 115\ mV$	
$V_K = -12\ mV$	
$V_l = 10.6\ mV$	
$V_{rest} = 0.0\ mV$	

*R_m is only used for simulating passive membrane compartments.

Received for publication 25 June 1990 and in final form 13 August 1990.

REFERENCES

Barron, D. H., and B. H. C. Matthews. 1935. Intermittent conduction in the spinal cord. *J. Physiol. (Lond.)*. 85:73–103.

Brigant, J. L., and A. Mallart. 1982. Presynaptic currents in mouse motor endings. *J. Physiol. (Lond.)*. 333:619–636.

Brill, M. H., S. G. Waxman, J. W. Moore, and R. W. Joyner. 1977. Conduction velocity and spike configuration in myelinated fibres: computed dependence on internode distance. *J. Neurol. Neurosurg. Psychiatry*. 40:769–774.

Brown, A. G., and R. E. W. Fyffe. 1978. The morphology of group Ia afferent fibre collaterals in the spinal cord of the cat. *J. Physiol. (Lond.)*. 274:111–127.

Brown, A. G., and R. E. W. Fyffe. 1979. The morphology of group Ib afferent fibre collaterals in the spinal cord of the cat. *J. Physiol. (Lond.)*. 296:215–228.

Bunow, B., I. Segev, and J. W. Fleshman. 1985. Modeling the electrical behavior of anatomically complex neurons using a network analysis program: excitable membrane. *Biol. Cybern.* 53:41–56.

Burke, R. E., B. Walmsley, and J. A. Hodgson. 1979. HRP anatomy of group Ia afferent contacts on alpha motoneurones. *Brain Res.* 160:347–352.

Chung, S., S. A. Raymond, and J. Y. Lettvin. 1970. Multiple meaning in visual units. *Brain Behav. Evol.* 3:72–101.

Deschênes, M., and P. Landry. 1980. Axonal branch diameter and spacing of nodes in the terminal arborization of identified thalamic and cortical neurons. *Brain Res.* 191:538–544.

Fyffe, R. E. W., and A. R. Light. 1984. The ultrastructure of group Ia afferent fiber synapses in the lumbosacral spinal cord of the cat. *Brain Res.* 300:201–209.

Goldstein, S. S., and W. Rall. 1974. Changes of action potential shape and velocity for changing core conductor geometry. *Biophys. J.* 14:731–757.

Grossman, Y., I. Parnas, and M. E. Spira. 1979*a*. Differential conduction block in branches of a bifurcating axon. *J. Physiol. (Lond.)*. 295:283–305.

Grossman, Y., I. Parnas, and M. E. Spira. 1979*b*. Ionic mechanisms involved in differential conduction of action potentials at high frequency in a branching axon. *J. Physiol. (Lond.)*. 295:307–322.

Hatt, H., and D. O. Smith. 1976. Synaptic depression related to presynaptic axon conduction block. *J. Physiol. (Lond.)*. 259:367–393.

Hirning, L. D., A. P. Fox, E. W. McCleskey, B. M. Olivera, S. A. Thayer, R. J. Miller, and R. W. Tsien. 1988. Dominant role of N-type Ca^{2+} channels in evoked release of norepinephrine from sympathetic neurons. *Science. (Wash. DC)*. 239:57–61.

Hodgkin, A. L., and A. F. Huxley. 1952. A quantitative description of membrane current and its application to conduction and excitation in nerve. *J. Physiol. (Lond.)*. 117:500–544.

Ito, M., and I. Takahashi. 1960. Impulse conduction through spinal ganglion. *In* Electrical Activity of Single Cells. Y. Katsuke, editor. Ikagu Shoin, Tokyo. 159–179.

Kennedy, D., and D. Mellon. 1964. Synaptic activation and receptive fields in crayfish interneurons. *Comp. Biochem. Physiol.* 13:275–300.

Khodorov, B. I., Y. N. Timin, S. Y. Vilenkin, and F. B. Gul'ko. 1969.

Theoretical analysis of the mechanisms of conduction of a nerve pulse over an inhomogeneous axon. I. Conduction through a portion with increased diameter. *Biofizika.* 14:304–315.

Krnjević, K., and R. Miledi. 1959. Presynaptic failure of neuromuscular propagation in rats. *J. Physiol. (Lond.).* 149:1–22.

Lindgren, C. A., and J. W. Moore. 1989. Identification of ionic currents at presynaptic nerve endings of the lizard. *J. Physiol. (Lond.).* 414:201–222.

Lüscher, H.-R., and J. S. Shiner. 1990. Simulation of action potential propagation in complex terminal arborizations. *Biophys. J.* 58:1389–1399.

Lüscher, H.-R., P. Ruenzel, and E. Henneman. 1979. How the size of motoneurones determines their susceptibility to discharge. *Nature. (Lond.).* 282:859–861.

Lüscher, H.-R., P. Ruenzel, and E. Henneman. 1982. Composite EPSPs in motoneurons of different sizes before and during PTP: implications for transmission failure and its relief in Ia projections. *J. Neurophysiol. (Bethesda).* 49:269–289.

Macagno, E. R., K. J. Muller, and R. M. Pitman. 1987. Conduction block silences parts of chemical synapse in the leech central nervous system. *J. Physiol. (Lond.).* 387:649–664.

Mallart, A. 1985. A calcium-activated potassium current in the motor nerve terminals of the mouse. *J. Physiol. (Lond.).* 368:577–591.

Parnas, I. 1972. Differential block at high frequency of branches of a single axon innervating two muscles. *J. Neurophysiol. (Bethesda).* 35:903–914.

Parnas, I., and I. Segev. 1979. A mathematical model for conduction of action potentials along bifurcating axons. *J. Physiol. (Lond.).* 295:323–343.

Parnas, I., M. E. Spira, R. Werman, and F. Bergman. 1969. Nonhomogeneous conduction in giant axons of the nerve cord of *Periplaneta americana. J. Exp. Biol.* 50:635–649.

Perney, T. M., L. D. Hirning, S. E. Leeman, and R. J. Miller. 1986. Multiple calcium channels mediate neurotransmitter release from peripheral neurons. *Proc. Natl. Acad. Sci. USA.* 83:6656–6659.

Quick, D. C., W. R. Kennedy, and L. Donaldson. 1979. Dimensions of myelinated nerve fibers near the motor and sensory terminals in cat tenuissimus muscles. *Neuroscience.* 4:1084–1096.

Rall, W. 1959. Branching dendritic trees and motoneuron membrane resistivity. *Exp. Neurol.* 1:492–527.

Raymond, S. A., and J. A. Lettvin. 1978. Aftereffects of activity in peripheral axons as a clue to nervous encoding. *In* Physiology and Pathobiology of Axons. S. G. Waxman, editor. Raven Press Ltd., New York. 203–225.

Revenko, S. V., Y. N. Timin, and B. I. Khodorov. 1973. Special features of the conduction of nerve impulses from the myelinized part of the axon to the non-myelinated terminal. *Biofizika.* 18:1074–1078.

Rinzel, J. and W. Rall. 1974. Transient response in a dendritic neuron model for current injection at one branch. *Biophys. J.* 14:759–790.

Schiller, Y., and R. Rahamimoff. 1989. Neuromuscular transmission in diabetes: response to high-frequency activation. *J. Neurosci.* 9:3709–3719.

Segev, I., J. W. Fleshman, J. P. Miller, and B. Bunow. 1985. Modeling the electrical behavior of anatomically complex neurons using a network analysis program: passive membrane. *Biol. Cybern.* 53:27–40.

Smith, D. O. 1980. Mechanisms of action potential propagation failure at sites of axon branching in the crayfish. *J. Physiol. (Lond.).* 301:243–259.

Smith, D. O. 1983*a*. Extracellular potassium levels and axon excitability during repetitive action potentials in crayfish. *J. Physiol. (Lond.).* 336:143–157.

Smith, D. O. 1983*b*. Axon conduction failure under in vivo conditions in crayfish. *J. Physiol. (Lond.).* 344:327–333.

Spira, M. E., Y. Yarom, and I. Parnas. 1976. Modulation of spike frequency by regions of special axonal geometry and by synaptic inputs. *J. Neurophysiol. (Bethesda.).* 39:882–899.

Stockbridge, N. 1988*a*. Differential conduction at axonal bifurcations. II. Theoretical basis. *J. Neurophysiol. (Bethesda).* 59:1286–1295.

Stockbridge, N. 1988*b*. Theoretical response to trains of action potentials of a bifurcating axon with one short daughter branch. *Biophys. J.* 54:637–641.

Stockbridge, N., and L. L. Stockbridge. 1988. Differential conduction at axonal bifurcations. I. Effect of electrotonic length. *J. Neurophysiol. (Bethesda).* 59:1277–1285.

Swadlow, H. A., J. D. Kocsis, and S. G. Waxman. 1980. Modulation of impulse conduction along the axonal tree. *Annu. Rev. Biophys. Bioeng.* 9:143–179.

Van Essen, D. C. 1973. The contribution of membrane hyperpolarization to adaptation and conduction block in sensory neurones of the leech. *J. Physiol. (Lond.).* 230:509–534.

Vladimirescu, A., K. Zhang, A. R. Newton, D. O. Pederson, and A. Sangiovanni-Vincentelli. 1981. SPICE Version 2G User's Guide. Department of Electrical Engineering and Computer Sciences, University of California, Berkeley.

Waxman, S. G. 1972. Regional differentiation of the axon: a review with special reference to the concept of the multiplex neuron. *Brain Res.* 47:269–288.

Waxman, S. G. 1975. Integrative properties and design principles of axons. *Int. Rev. Neurobiol.* 18:1–40.

Waxman, S. G., and M. H. Brill. 1978. Conduction through demyelinated plaques in multiple sclerosis: computer simulations of facilitation by short internodes. *J. Neurol. Neurosurg. Psychiatry.* 41:408–416.

Waxman, S. G., and R. J. Melker. 1971. Closely spaced modes of Ranvier in the mammalian brain. *Brain Res.* 32:445–448.

Waxman, S. G., and S. L. Wood. 1984. Impulse conduction in homogeneous axons: effects of variation in voltage-sensitive ionic conductances on invasion of demyelinated axon segments and preterminal fibers. *Brain Res.* 294:111–122.

Westerfield, M., R. W. Joyner, and J. W. Moore. 1978. Temperature-sensitive conduction failure at axon branch points. *J. Neurophysiol. (Bethesda).* 41:1–8.

Yau, K.-W. 1976. Receptive fields, geometry and conduction block of sensory neurones in the central nervous system of the leech. *J. Physiol. (Lond.).* 263:513–538.

Zucker, R. S. 1974. Excitability changes in crayfish motoneuron terminals. *J. Physiol. (Lond.*). 241:111–126.